17th World Conference on Earthquake Engineering, 17WCEE
Sendai, Japan - September 13th to 18th 2020

SEISMIC VULNERABILITY ASSESSMENT OF INTEGRAL ABUTMENT BRIDGE WITH AND WITHOUT SLEEVED PILE

A. Lego [(1)], A. Dutta [(2)] and S.K. Deb[(3)]

[(1)] *Research Scholar, IIT Guwahati, atoplego@gmail.com*
[(2)] *Professor, IIT Guwahati, adutta@iitg.ac.in*
[(3)] *Professor, IIT Guwahati, skdeb@iitg.ac.in*

Abstract

Seismic performances of Integral Abutment Bridges (IAB) are superior due to redundant frame type configuration of bridge as compared to the conventional bridge with joints and bearings at piers and abutments. Further, the flexibility in the substructure and foundation of IAB plays key role in enhancing the performance of the bridge under seismic excitation by lengthening the vibration period of the bridge. In the present study, improvement in the seismic performance of IAB is observedby further increasing the flexibility of foundation through introduction of sleeved pile foundation. Comparative study of seismic performance of IAB is carried out using incremental dynamic analysis of the IAB with and without sleeved pile and the seismic vulnerabilities are assessed at different damage states by developing fragility curves.

Keywords: integral abutment bridge, incremental dynamic analysis, damage states, fragility curve.

1. Introduction

The Integral Abutment Bridges (IAB) are designed and constructed without movable deck joints at piers or abutments. These are either single span or multiple spans with the superstructure cast integrally with the abutment. In the case of multiple span IAB, the superstructures are supported either on flexible pier with deck integrated to the pier or on a rigid pier with bearing supporting the deck. The backfill behind the abutment forming the part of approach to the bridge confine the bridge from both ends. Due to such configuration of the of bridge, the deformation caused by external load due to seismic excitation, vehicular load and thermal load on the bridge deck spreads throughout the supports, which are rigidly connected to the deck. Therefore, the flexibility in the substructure and foundation of IAB play key role in enhancing the performance of the bridge under seismic excitation and thermal load. The seismic performance of IAB are also superior due to redundant frame type configuration of the bridge as compared to the conventional bridge with joints and bearing at pier and abutment. In addition, further enhancement in the performance of IAB under external load can be achieved through the strategies of lengthening the vibration period by introducing flexibility in the foundation by adopting sleeved pile. The sleeved pile is comprised of a pile within a sleeve having inner diameter substantially larger than the outer diameter of the pile to allow free lateral movement of the pile within the sleeve. The pile inside the sleeve is supported either by embedding in the bottom concrete pile extended up to some depth below the pier cap or by pile to sleeve connection at discrete points along the elevation. The principal function of the sleeve is to provide a pile of unsupported length, thereby achieving flexible and low stiffness response to horizontal loading. Boardman et al. [1] adopted a concept of the sleeved pile in the construction of the Union House, New Zealand with prime objective of minimizing ductility demand of each individual member in the superstructure. Consequently, deriving the motivation from the increase in flexibility of structure by use of sleeved pile, the foundation of IAB under consideration in this study is designed with sleeved pile for enhancing the performance of the IAB under seismic excitation. Further, the appreciation of the distinctive performance level of IAB with and without sleeved pile under seismic excitation is carried out by analyzing a three-dimensional finite element model of IAB with and without sleeved pile, incorporating soil pile and abutment backfill interaction. In the modelling of the soil pile interaction of IAB without sleeved pile, the lateral soil pile interaction in pile supporting abutment and pier are modelled using load deflection p-y curve, the tip bearing interaction of the pile is modelled using load settlement Q-z curve and the shaft frictional resistance of the pile is modelled using load movement t-z curve. The abutment backfill interaction is modelled using the relation between the passive pressure mobilized and wall movement. In the case of the modelling of soil pile interaction of IAB with sleeved pile the modification is made only in the modelling of lateral soil pile interaction by removing the p-y curve soil spring from the sleeve portion of sleeved pile foundation. This is because of the fact the at the sleeve length housed in the casing of the sleeved pile do not come in contact with the surrounding soil to experience resistance to lateral deflection from the soil.

The analyses for comparing the performance level of the IAB with and without sleeved pile are carried out by adopting the incremental dynamic analysis (IDA) and the comparative seismic vulnerability is assessed through fragility function. The IDA provides a parametric analysis method to more thoroughly estimate the structural performance under seismic load [2]. It involves subjecting a structural model to one or more ground motion records, each scaled to multiple levels of intensity, thus producing one or more curves of response vs. intensity level. The IDA provides a thorough evaluation of the seismic response for a wide range of seismic intensity level corresponding to different damage states from yielding up to collapse. The comparison of the vulnerability of the IAB with and without sleeved pile is carried out by developing analytical fragility curve for the bridge categories. Different damage states of pier such as yielding, concrete cover spalling and bar buckling are defined in the terms of drift of the pier. The median seismic demand for each damage states is estimated by interpolation of IDA results. Assuming the demand and capacity of the bridge to follow lognormal distribution, the comparative fragility curve for each damage state is plotted for both the categories of bridge and their performance levels are compared. No literature on such comparative studies on distinctive performance level of IAB with and without sleeved pile is observed. Hence this study would be significantly beneficial to bridge design engineer for planning and design of IAB with enhanced seismic capacity in high seismic risk areas for important transportation corridors.

2. Description of bridge

An IAB with a total length of 120 m, having two end spans of 37.50 m and one central span of 45 m is considered. The deck of the bridge consists of a concrete slab of 250 mm thickness supported by four numbers of longitudinal steel plate girders. The connections between the deck slab and steel girders are achieved through shear connectors. Diagonal bracing of girders are provided at 5000 mm intervals along the span. The abutment wall at both ends of the bridge is 1000 mm thick with overall height of 5000 m. Circular piers of 1500 mm with clear height of 4000 mm up to the bottom level of pier cap are used. Rigid connections between the girder ends and abutment are ensured by encasing the ends of all the girders into the abutment wall. The rigid connection between the pier and the girder is achieved through hold down bolts encased in the pier cap. The general arrangement drawing of the bridge is shown in Fig.1.

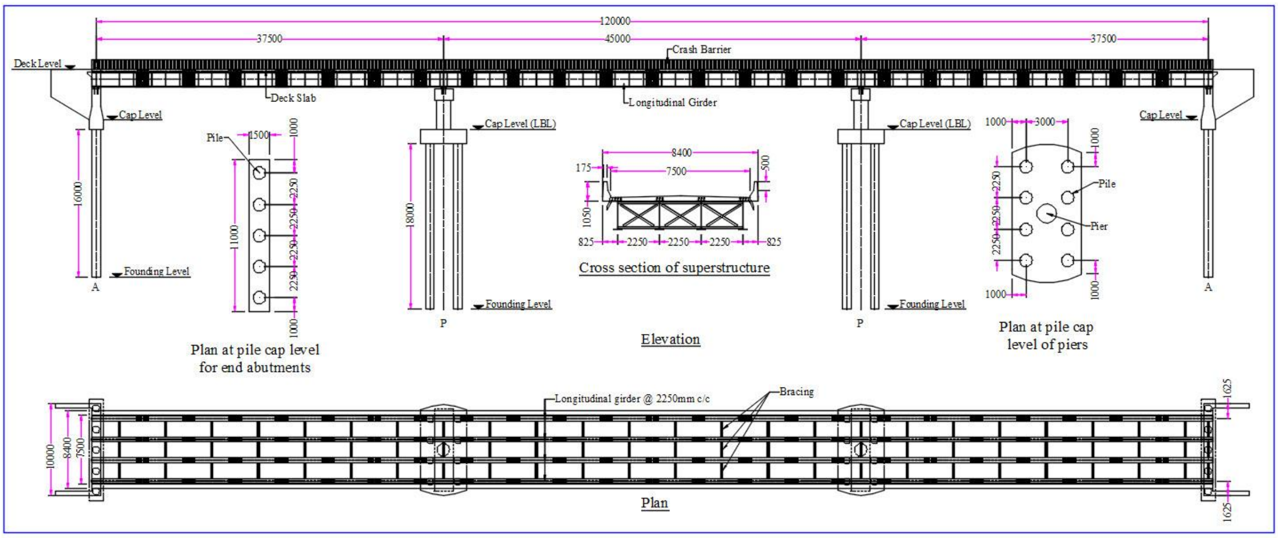

Fig. 1 – General arrangement drawing of IAB

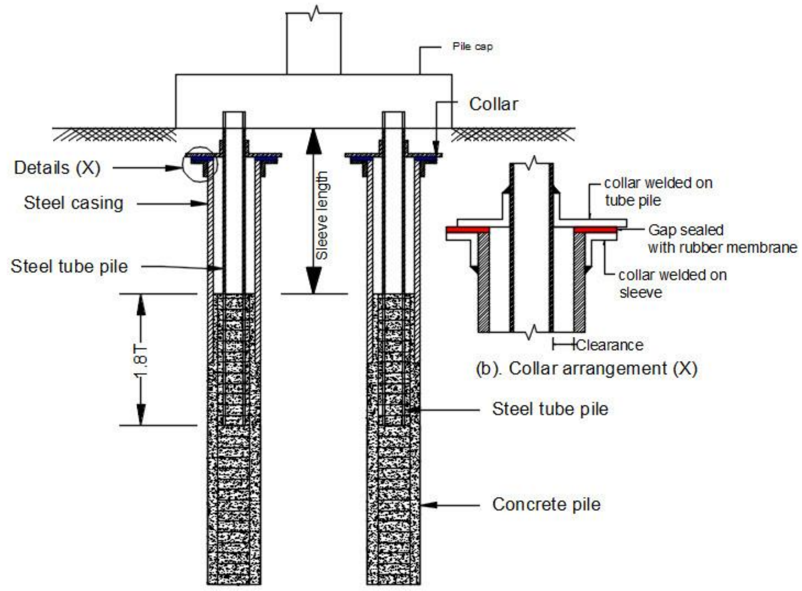

Fig. 2 – Proposed of arrangement of sleeved pile for bridge in the present study

In the IAB without sleeved piles, each abutment is supported on five numbers of concrete piles of 900 mm diameter arranged in a single row and the piers are supported on eight piles of 900 mm diameter arranged in two rows with a pile cap of 1500 mm thick slab. The characteristic strength of concrete adopted in abutment wall is 30 MPa with main rebar of 0.8% and confining rebar of 0.5% of gross area. Similarly, the characteristic strength of concrete adopted in pier and piles is 35 MPa with main rebar of 1.4% and confining rebar of 0.3% of gross area in pier and main rebar of 2.0% and confining rebar of 0.3% in piles respectively. The structural arrangement of the sleeved pile adopted in the foundation of IAB in the present study consists of steel tube pile at upper portion and concrete pile in the bottom portion supporting the steel tube. The diameter of the concrete pile shall be substantially larger than that of the outer diameter of the steel tube pile. The bottom end of the steel tube pile shall be embedded in to the bottom concrete pile up to a designed depth and the top end shall be embedded into the pile cap. The portion of steel tube pile from the top of concrete pile to the bottom level of pile cap shall be sleeved inside a steel casing as shown in Fig. 2.

3. Finite Element Modelling of Bridge

The bridge superstructure of IAB is modelled in using grillage model since the long composite steel girder and concrete deck slab may not behave as fully rigid deck [3]. The deck of the bridge is thus idealized as a series of longitudinal and transverse beam elements interconnected at the nodes. The longitudinal steel composite girder is modelled with longitudinal grillage beam with the stiffness properties of the composite section taking the effective width of the reinforced concrete deck slab into account. The deck slab of the bridge is modelled by transverse grillage beam with the depth of the beam equal to the thickness of the deck and width of the beam equal to the spacing of the transverse beam. The portion of the effective width of the deck slab modelled along with the steel girder in the longitudinal direction is transformed to an equivalent steel section through the modular ratio of steel and concrete and is assigned a massless material since the seismic weight or mass of the portion of the effective width of the reinforced concrete deck slab is considered in the modelling of the deck slab using transverse grillage beam.

The superstructure of the bridge is long compared to the width and depth of the girder and is assumed to respond elastically under lateral seismic loading [4]. Hence, the structural component of the superstructure is modelled with elastic properties of the materials.

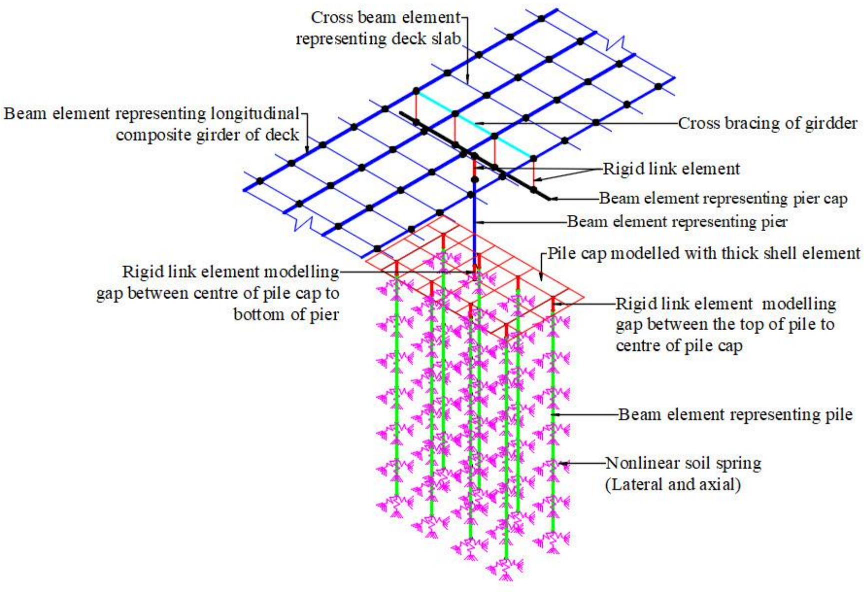

Fig. 3 – Schematic diagram for strategies of finite element modelling of bridge with soil pile interaction

Fig. 3 shows the schematic diagram for strategies in finite element modelling of the bridge with pile foundation. The total deck assembly is placed at the centroid of the composite deck in its location in elevation in the model. Similarly, the pier cap is also modelled with beam element and placed at it centroidal location in elevation. Therefore, gaps exist between the top of pier and pier cap located at is centroid and between the pier cap and the girders located at their respective centroids. The connection through these gaps are established by adopting rigid link elements. The abutment wall is modelled with thick shell element and the ends of the girders are connected to the abutment wall. The pier, pier cap and piles are modelled using beam element. The pile cap in pier foundation is modelled using thick shell element.

In the IAB with sleeved pile, the steel tube pile is modelled with beam element. The steel casing encasing the sleeve length is ignored in the modelling of sleeved pile as it do not have any contribution on the strength and stiffness of the sleeved pile. The concrete pile in the bottom portion of the sleeved pile is modelled as beam element.

In the present study, the comparison of performance level under seismic excitation is carried out on IAB with and without sleeved pile founded on medium sand. The engineering properties medium sand adopted in the modelling of soil pile interaction are as shown in Table 1.

Table 1 – Chemical composition of cement samples

Type of soil	**Modulus of elasticity (kPa)**	**Initial Modulus of subgrade reaction kN/m²/m**	**Angle of internal friction (φ)**	**Unit weight of soil (Y) kN/m³**	**Poisson's Ratio (v)**
Medium Sand	15000	21000	35^0	18	0.32

The piles supporting the abutments and piers are required to sustain axial as well as lateral loads. The axial load carrying capacity of a pile is a combination of the tip bearing capacity of the pile and the skin frictional resistance from the mobilized soil surrounding the pile. In the numerical model of the IAB, the pile tip bearing interaction with soil is modelled using load settlement (Q-z) curve as recommended in API (2007). Similarly, the interaction of the shaft frictional forces of the pile is modelled by adopting load movement (t-z) curve. The shaft frictional forces is considered negligible for a length of the pile equal to three times the diameter of piles L_0 from the bed level, since this portion of the pile length may have negligible over burden pressure or may be subjected to scouring [5].

The modelling of soil pile interaction under lateral load on pile is carried out by adopting the p-y curves which represent the lateral load deformation of soil under the laterally applied pressure on a discrete vertical segment of pile at any depth. In this study, the modelling of soil pile interaction of the laterally loaded pile is carried out by adopting the hyperbolic formulation as recommended in [6].

4. Selection of ground motion

The selection of ground motion is known to be an important consideration in the assessment of seismic capacity of structure, based on dynamic analysis. The primary objective of IDA is to study the relative capacity of the bridge categories under seismic excitation without consideration to site specific seismic hazard. Therefore, the selection of ground motion records has been selected using AR method [7] in which the records are selected arbitrarily without any attempt to match any specific properties of the record. In addition, the limit specified by Haselton and Deielerion [8] to ensure that the ground motion selected consist ofstrong motions representing an extreme event that may cause the collapse of the structure is taken into consideration while selecting the ground motion records. Thus, the selected ground motion has magnitude (M) > 6.5, distance from source to site(R) >10 km, peak ground acceleration > 0.2g and peak ground velocity >15cm/sec. The list of 20 ground motion records selected for the IDA in this study is as given in Table 1. These selected ground motion have been downloaded from the library of ground motion in website of Consortium of Organization for Strong Motion Observation Systems (COSMOS) [9].

Table 2 – List of ground motion records selected for IDA

SL No	Earthquake ground motion	M	PGA (g)	R (km)
1	Cape Mendocino, USA,1992	7.2	0.492	49.10
2	Chamoli, India,1999	6.6	0.359	12.30
3	Chi Chi, Taiwan,1999	7.6	0.361	24.70
4	Imperial valley, USA,1979	6.5	0.242	10.60
5	Imperial Valley, USA,1978	6.5	0.273	10.40
6	Indian Burma Border,1998	7.2	0.224	189.90
7	Indian Burma Border,1998	7.2	0.282	210.10
8	Kobe, Japan,1998	6.9	0.344	22.50
9	Lander, (2217) USA,1992	7.3	0.284	10.00
10	Lander USA,1992	7.3	0.222	31.00
11	Limon, Costarica,1991	7.5	0.261	10.00
12	Loma Priesta, USA,1989	7.5	0.398	14.30
13	Manjil, Iran,1990	7.4	0.496	12.60
14	Northridge, USA,1971	6.6	0.325	12.20
15	Northridge, USA,1971	6.6	0.354	23.50
16	Sand Fernando, USA,1971	6.6	0.254	16.50
17	Sand Fernando, USA,1971	6.6	0.213	23.10
18	Sand Fernando, USA,1971	6.6	0.283	19.80
19	Superstition Hill,USA ,1987	6.6	0.255	18.20
20	Uttarkashi, India1991	7.0	0.359	34.00

5. Damage States Modelling of IAB

The literatures on assessment of seismic vulnerability of bridge using fragility function indicates a trend of component level approach in which the contribution of the major bridge components such as pier, abutment and bearing are considered in the development of overall bridge system fragility.

Table 3 – Damage state for the bridge pier considered in present study

Damage state	Drift ratio (%)	Description of damage state
Yielding (Serviceable) (DS1)	0.57	Initiation of cracks in cover concrete
Concrete cover spalling (DS2)	1.88	Spalling of cover concrete; strength may continue to increase.
Bar buckling (DS3)	4.37	Hoop fracture, buckling of longitudinal bar. degradation of strength by cracking of core concrete

In the present study, three damage states are adopted in the comparative study of the performance level under seismic excitation of the IAB with and without sleeved pile. The damage states are: Yielding

(DS1), Concrete cover spalling (DS2) and Bar buckling (DS3). The drift ratio on the onset of the yielding is computed from the yield curvature-displacement relationship given by Priestly et al. [10]. The drift ratio on the onset of concrete cover spalling and bar buckling is calculated as per Berry and Eberhard [11]. The drift ratio computed at the damage state for the bridge pier in the present study with an effective height of 4.00 m and a diameter of 1.5 m are as shown in Table 3.

6. Performing Incremental Dynamic Analysis

In order to identify the performance level of IAB with and without sleeved pile, the IDA on the models of IAB is performed by applying the excitation of the selected ground motion as shown in Table 1 along the transverse direction. Each record is scaled to cover the entire range of the structural response from elasticity to the yielding and finally to the collapse of the bridge. In the present analyses, the PGA and drift of pier is adopted as corresponding IM and DM. In the initial stage of analysis, one or two elastic runs are carried out by scaling the IM level of the ground motion in the range of 0.10g to 0.15g [2]. In the subsequent run, the ground motion records are stepped up with 0.05g time the number of run up to the step under consideration. The analysis with stepping up of IM is stopped when collapse state is indicated. In order to ensure that the IM at which the model collapses are the lowest IM at which the bridge pier collapses under the corresponding ground motion, a confirmatory analysis is carried. This confirmatory analysis is done by taking an IM value in between the maximum IM value at which the model has collapsed and its next lower value. In the event of collapse at lower IM during a confirmatory analysis, the lower value is considered as the IM at which the bridge pier shall collapse under the considered ground motion. The drift of pier (DM) are obtained from the results of the analysis and the corresponding PGA (IM) at every step of the analysis with a ground motion is recorded. Using the set of IM and DM values from series of analyses on the bridge model, the IDA curve for the IAB with and without sleeved pile is generated for ground motions as shown in Figs. 4 (a) & (b).

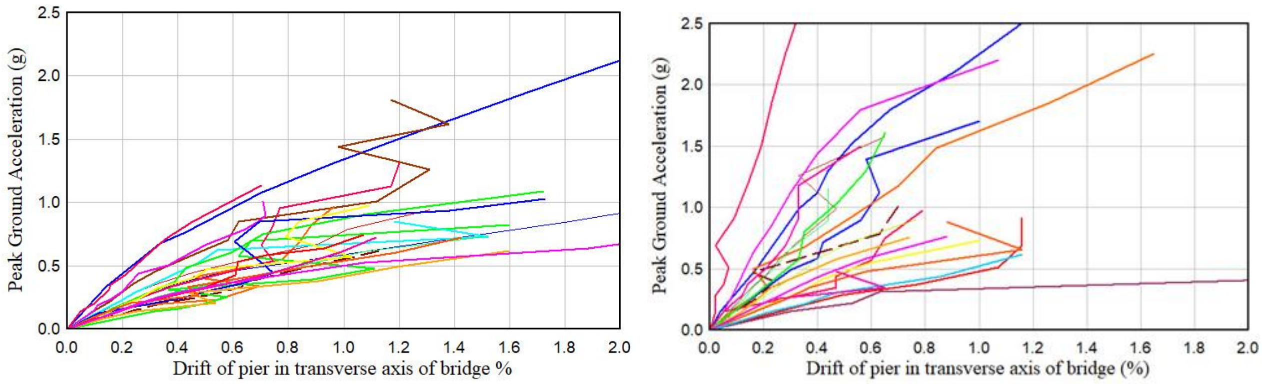

(a) (b)

Fig. 4 – IDA curve of IAB (a) without sleeved pile (b) with sleeved pile

The IDA curve of IAB with and without sleeved pile as shown in Figs. 4 (a) & (b) indicate a distinct elastic linear region at lower IM. The linearity of different curves terminates at different IM and afterwards the majority of the curves soften. This depicts the behavior of the structure with initially linearly elastic elements. However, some of the IDA curves shown in Figs. 4 (a) & (b) displays successive softening and hardening. The stiffness of some curves decreases with higher IM while that of some others increase. Such behavior is observed more in the IDA of the bridge with sleeved pile. Vamvatsikos and Cornell [12] observed that it is the pattern and timing that also makes a difference in the response of the elastoplastic system rather than only by IM. As the accelerogram is scaled up, the weak response cycle in the early part of the time history response becomes strong enough to inflict damage and alter the properties of the structures subjected to the stronger cycles. The configuration of IAB with sleeved pile in foundation is different from the IAB without sleeved pile. Therefore, the presence of more curves with wavy character in the IDA curve of IAB with sleeved pile can be attributed to the difference in the configuration of the foundation, thus modifying the dynamic characteristics of the bridge.

By the interpolation of IDA curve pertaining to each ground motion record, the IDA results can be expressed in any IM. The extracted *IM* and *DM* values from each nonlinear dynamic analysis forming a set of discrete point for each record is interpolated for use in generating additional *IM* or *DM* values without additional analysis. Complex spline to simpler linear interpolation methods are adopted in the process. Mander et al. [13] observed that interpolation using multiple spline function is cumbersome and not particularly useful for subsequent risk analysis. From the result of exploring several single functions for use in interpolation method, Mander et al. [13] also observed the Ramberg-Osgood equation as the most suitable. Therefore, in the present analysis, the Ramberg – Osgood (R-O) equation is adopted for the interpolation of the IDA data which is given as (Mander et al. 2007).

$$\frac{EDP}{EDP_c} = \frac{IM}{IM_c} + \left(\frac{IM}{IM_c}\right)^r = \frac{IM}{K_e \times EDP_c}\left(1 + \left|\frac{IM}{IM_c}\right|^{r-1}\right) \tag{1}$$

where, K_e is the initial slope of IDA curve in proportional range, IM_c is the critical intensity measure that occurs at the onset of large EDP that leads to subsequent collapse, EDP_c ($EDP_c = IM_c /K$) is the critical value of *EDP* and *r* is a constant. In the initial interpolation process, the value of *r* for each pair of the *IM* and *DM* in each step of the analysis for each ground motion is calculated. Further, using the median value of *r* for each ground motion, interpolation value of *IM* or *DM* for the ground motion is carried out. During the interpolation, it has been found that the value of *r* in R-O relation varies across the suite of IDA curve of ground motions. Mander et al. [13] also observed the same variation in the seismic risk analysis of a bridge and hence adopted a fixed value of *r*, such as 12 for the New Zealand code, 6 for the Japanese code and 6 for Caltrans in a seismic risk assessment analysis. In the present study also, the value of *r* is observed to be varying across the suit of IDA curve. Hence, the value of *r* adopted as 5 which is observed to be optimally fitting to the IDA curves generated in the analysis and adopted in the interpolation of *IM* or *DM* values for the all ground motions.

Furthermore, the scattered *DM* values in IDA curves are summarized to their 16%, 50% and 84% percentiles [2]. To carry out the summarization of DM values, stripes of DM at arbitrary IM values are interpolated for each ground motion using R-O Eq. (1). The value of K_e, IM_c and EDP_c for respective ground motion is adopted in the interpolation of *DM* values at a given *IM*. Therefore, each stripe of the *DM* for a given *IM* contains 20 *DM* values representing each ground motion. By summarizing the DM values for each stripe into their 16%, 50% and 84% percentile, the DM values for given *IM* are interpolated for each fractiles to generate 16%, 50% and 84% of IDA curves. The summary of the IDA curve for IAB without and with sleeved pile for *DM* values given IM is shown in Figs. 5 (a) & (b). Using the summary of IDA shown in Fig. 5 (a) for IAB without sleeved pile, it is interpolated as for damage state DS1 the corresponding PGA for 16% fractiles of DM is 0.605g, 50% fractiles of DM is 0.40g and 84% fractiles of DM is 0.305g.

Therefore, the demand for the damage state is interpolated as: for DS1, 84% of the records is to be scaled to PGA ≥ 0.305g or 50% of the records to PGA ≥ 0.40g or 16% of the records to PGA ≥ 0.605g [14]. Thus, the median demand for DS1 works out to 0.4g which is the *IM* corresponding to $DM_{50\%}$. Table 4 shows the demand interpolated using summary of IDA curve as shown in Figs. 5 (a) & (b).

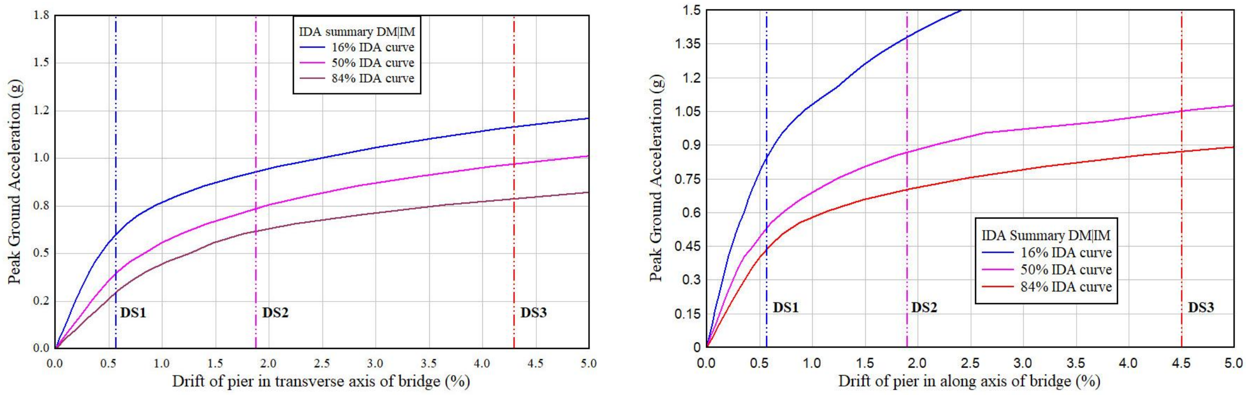

(a) (b)

Fig. 5 – The summary of IDA curve into 16%, 50%. 84% fractiles of *DM* for IAB (a) without sleeved pile (b) with sleeved pile

Table 4 –Demand interpolated for IAB with and without sleeved pile in terms of PGA against the fractiles of DM from IDA curve

Damage state	IAB without Sleeved Pile			IAB with Sleeved Pile		
	Corresponding PGA(g)			Corresponding PGA (g)		
	$IM_{16\%}$	$IM_{50\%}$	$IM_{84\%}$	$IM_{16\%}$	$IM_{50\%}$	$IM_{84\%}$
DS1	0.605	0.40	0.305	1.20	0.60	0.35
DS2	0.93	0.72	0.61	>1.8	1.10	0.70
DS3	1.15	0.97	0.78	>1.8	1.30	0.90

In addition, the median IDA curve of the bridge computed taking the median values of K_e, IM_c and EDP_c of 20 ground motions is adopted in the IDA. The interpolation of the IDA curve for arbitrary values of *IM* is done using R-O equation (Equation 1). Fig. 6 shows the median IDA curve of IAB with and without sleeved pile. The median curve indicates that the median seismic demand of the IAB with sleeved pile for different damage states is higher than that of IAB without sleeved pile. This indicates superior performance level of IAB with sleeved pile under seismic excitation.

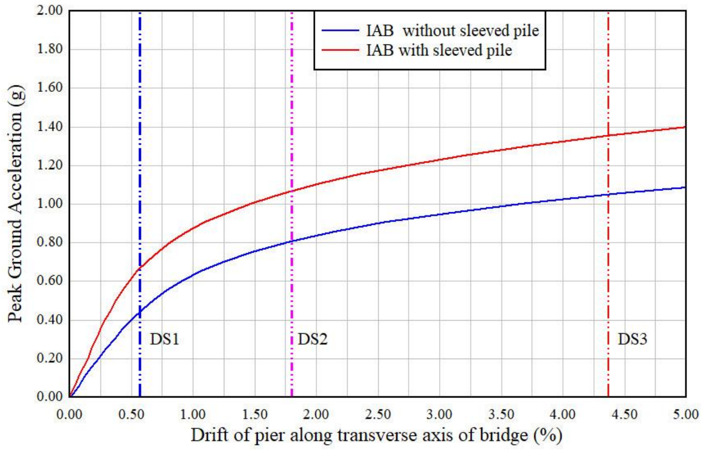

Fig. 6 – Median IDA curve of the IAB without and with sleeved pile from R-O Equation

7. Seismic Fragility Analysis of IAB without and with Sleeved Pile

In this current study, the seismic fragility analysis of the bridge is carried out using the analytical method. The fragility curve of the bridge, which is the conditional probability state of the bridge's vulnerability as a function of ground motion, is a common tool for seismic vulnerability assessment. The configuration of the bridge considered in the study indicates that the bridge will lose its function only if there is damage to the pier. Hence, the seismic fragility analysis is carried out considering the damage states of the pier.

The seismic fragility identifies the probability that the seismic demand on the structure (*D*) is greater than the capacity. The probability is conditioned on a chosen intensity measure (*IM*) which represents the level of seismic loading. The representation of this conditional probability is given as [15]:

$$Fragility = P\left[D \geq C \middle| IM\right] = P\left[C - D \leq 0.0 \middle| IM\right] \quad (2)$$

The solution of the Eq. (2) is accomplished through seismic demand obtained using IDA. Assuming that the demand and capacity of the structure to follow lognormal distribution, the fragility statement in Eq. (2) takes the following form as [15]:

$$P\left[D > C \middle| IM\right] = \phi\left(\frac{\ln\left(S_d / S_c\right)}{\sqrt{\beta_{D|IM}^2 + \beta_c^2}}\right) \quad (3)$$

Taking the value of S_d (the median estimate of demand), S_c (median estimate of the capacity), $\beta_{D|IM}$ (the dispersion or logarithmic standard deviation of the demand conditioned on the intensity measure) and β_c (the dispersion of the capacity), the fragility curve of the bridge is developed. In the estimation of uncertainty in the seismic demand $\beta_{D|IM}$ of bridge pier, Stefanidou and Kappos [16] observed its value to be varying and increase with the higher level of intensity. It was also observed that uncertainty in seismic demand may be equal, greater, or even less than value recommended in HAZUS. The HAZUS [17] specifies a dispersion value of 0.60 for ground shaking algorithm of damage function of bridge. In the present study, for the purpose of comparative evaluation of the bridge type with and without sleeved pile, the value of $\beta_{D|IM}$ is taken as 0.6 in the line of dispersion value specified in HAZUS [17]. In addition, the value of dispersion of capacity is adopted as 0.35 for pier in the line of representative value proposed by Stefanidou and Kappos [16] in their studies of the development of bridge specific fragility curves.

Furthermore, the median demand for the different damage state is obtained from the summarized curve of IDA to various percentiles of *DM*. The PGA value corresponding to the damage state at 50% percentile of *DM* that is $IM_{50\%}$ is adopted as the median demand of the damage state. The value of median demand for various damage state adopted in the development of fragility curve for different damage state is shown in Table 5.

Table 5 – Estimated median IM values from IDA summarization

Bridge type	**Median *IM* for different damage states (g)**		
	DS1	**DS2**	**DS3**
IAB without sleeved pile	0.4	0.72	0.97
IAB with sleeved pile	0.6	1.10	1.3

The comparative plot of the fragility curve developed for IAB and SIAB with and without sleeved pile using the median demand is shown in Figs. 7 (a)-(c).

The comparative study of the fragility curves of IAB with and without sleeved pile distinctively indicates that the bridge with sleeved pile is less vulnerable under different damage states considered. The ground acceleration required for initiating probability of exceedance of damage states in the bridge with sleeved pile is observed to be marginally higher. This clearly signifies the improvement in seismic capacity of the bridge with sleeved pile.

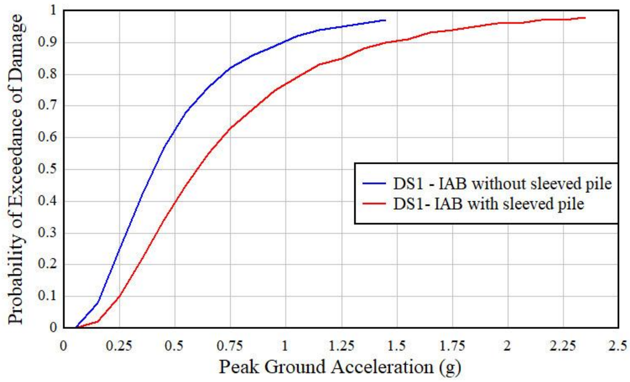

(a)

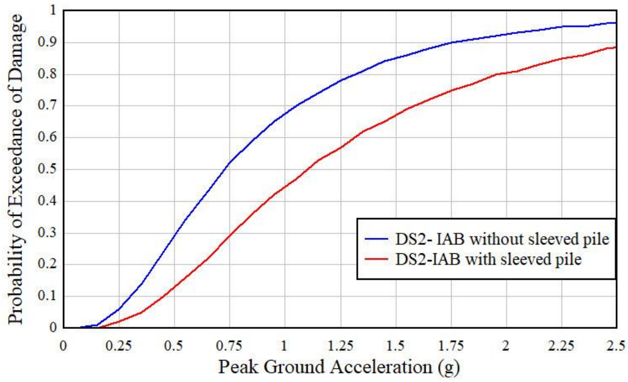

(b)

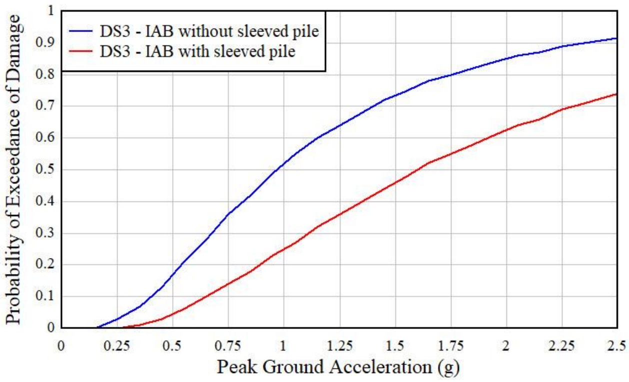

(c)

Fig. 7 – Fragility curve of IAB without and with sleeved pile (a) DS1 (b) DS2 and (c) DS3

8. Concluding Remarks

From the finite element modelling, IDA results and fragility curve of IAB with and without sleeved pile, the conclusions are as follows:

1. The arrangement of sleeved pile is an effective means of controlling seismic response of IAB. The seismic performance of the bridge improves with the adoption of sleeved pile in foundations of IAB and also increases the overall safety margin of the bridge. The sleeved pile can be considered as a durable isolation system for IABs constructed in high seismic risk areas.

2. Very good estimate of performance level of each category of bridge model can be achieved using IDA.

3. The IDA results and fragility curve of IAB with and without sleeved pile corresponding to different damage states indicate that the bridge with sleeved pile in foundation is less vulnerable to seismic excitation.

9. References

[1] Boardman PR, Wood BJ (1983): Union house - A crossed braced structure with energy dissipators. Bulletin of the New Zealand National Society for Earthquake Engineering, **16** (2), 83-97.

[2] Vamvastsiko D, Cornell CA (2004): Applied Incremental Dynamic Analysis. *Earthquake Spectra*, **20** (2), 523-553.

[3] CALTRANS (2015). Bridge Design Practice, Chapter 4, www.dot.ca.gov/des/techpubs/bdp.html.

[4] Priestly MJN, Calvi GM (1996): *Seismic Design and Retrofit of Bridges*. John Wiley & Son Inc, New York.

[5] FEMA-356 (2000). Pre-standard and commentary for the seismic rehabilitation of building, FEMA, Washington D.C.

[6] American Petroleum Institute (2007): Recommended practice for planning, designing and constructing fixed offshore platform – working stress design, Transportation Research Board, API Publishing Services, Washington D.C., USA.

[7] Baker JW and Cornell CA (2006): Spectral shape, epsilon and record selection, *Earthquake Engineering and Structural Dynamics*, **35**, 1077-1095.

[8] Haselton CB, Deierlein GG (2007): Assessing seismic collapse safety of modern reinforced concrete moment-resisting frame building. *Technical Report PEER-2007/08*, Pacific Earthquake Engineering Research Centre, University of California, Berkeley, USA.

[9] COSMOS (Consortium of Organization for Strong Motion Observation Systems) Virtual Data Center - Strong Motion Center, www.cosmos-eq.org.

[10] Priestly MJN, Calvi GM, Kowalsky MJ (2007): *Displacement-based seismic design of structures*. IUSS Press, Pavia, Italy.

[11] Berry MP, Eberhard MO (2007): Performance modelling strategies for modern reinforced concrete bridge columns. *Technical Report PEER-2007/07*, Pacific Earthquake Engineering Research Centre, University of California, Berkeley, USA.

[12] Vamvatsikos D, Cornell CA (2002): Incremental dynamic analysis. *Earthquake Engineering & Structural Dynamics*, **31** (3), 491-514.

[13] Mander JB, Dhakal RP, Mashiko N, Solberg KM (2007): Incremental dynamic analysis applied to seismic financial risk assessment of bridges. *Engineering Structures*, **29**, 2662-2672.

[14] Vamvastsiko D, Cornell CA (2002a): Incremental dynamic analysis and its application to performance-based earthquake engineering. *12th European Conference in Earthquake Engineering*, London, UK.

[15] Nelson BG, DesRoches R (2007): *Seismic fragility methodology for highway bridges using component level approach*. Journal of Earthquake Engineering & Structural Dynamics, **36**, 823-839.

[16] Stefanidou SP, Kappos AJ (2017): Methodology for the development of bridge specific fragility curves. Earthquake *Engineering & Structural dynamics*, **46**, 73-93.

[17] HAZUS-MH MR4 (2003): Multi-hazard loss estimation methodology earthquake mode (FEMA-2003). National Institute of Building Sciences, Washington D.C.

